Generation of Mode-Selective Frequency Response Functions from Temporally Sampled, Broadband and Multimodal Guided Ultrasonic Wave Signals

THOMAS ROLOFF and MICHAEL SINAPIUS

ABSTRACT

Structural health monitoring (SHM) systems for thin-walled, large-scale structures using guided ultrasonic waves (GUW) have recently been complemented by methods based on frequency response functions (FRF). These approaches enable the calculation of the structure's response to any artificially generated excitation signal within the frequency range under investigation.

This study presents a novel concept for extracting separate FRFs for the two fundamental modes from temporally sampled, broadband and multimodal GUW signals.

In this work, quasi-ideal impulse response functions (IRF) are generated by retransforming multimodal broadband FRFs into the time domain. These FRFs are recorded energy-efficiently using sweep excitation and contain all occurring GUW components at the sensing position. The extended dispersion based frequency-domain intrinsic component decomposition (DBFICD) algorithm and the iterative frequency-domain envelope-tracking filter (IFETF) algorithm are used to extract the corresponding signal components from the IRFs. Based on their different dispersive behaviour they can be assigned to the fundamental modes and combined to form the two respective IRFs. Transforming the latter back into the frequency domain results in two separate FRFs. This allows damage detection algorithms to estimate the structure's mode-selective response to any selected signal within the frequency range under investigation.

The method is validated experimentally by recording multimodal and single-mode FRFs in an aluminium plate with a mode-selective, two-sided piezoelectric actuator setup and a laser Doppler vibrometer. The estimated single-mode structural responses based on the FRFs extracted by the presented approach agree well with the actual responses to mode-selective excitation.

The presented concept enables mode-selective FRF-based SHM systems to work with multimodal excitation, which reduces setup complexity and increases the application range by providing information for both fundamental modes over a wide frequency range.

Thomas Roloff, Research Associate and PhD Student, Email: thomas.roloff@tu-braunschweig.de. Institute of Mechanics and Adaptronics, Technische Universität Braunschweig, Braunschweig, Germany

INTRODUCTION

Guided ultrasonic waves (GUW) are an efficient tool for monitoring thin-walled, large-scale structures with structural health monitoring (SHM) systems. The damage detection methods in these systems evaluate the wave propagation to detect, localise and identify damage based on reflections, scattering or amplitude attenuation [1].

GUW can travel over long distances and appear in at least two modes at any frequency [2, 3]. The symmetric S and asymmetric A modes differ in their phase velocities and thus wavelengths as well as their in-plane and out-of-plane components of the particle motion which is why they are predestined for investigating different kinds of damage [4, 5]. However, most damage detection algorithms investigate only one of the wave modes, as multimodal signals significantly reduce the performance of the damage detection [6]. In consequence, these methods need baseline measurements for eliminating one of the modes [6] or mode-selective excitation of the signals [5, 7]. The former assumes a damage free state of the structure for the baseline measurement and the latter requires complex actuator design or setups and is limited in frequency range [5].

Another approach for evaluating mode-selective data is the extraction of the respective mode components from sampled data. Methods evaluating the data in the frequency-wavenumber-domain rely on setups with a lot of spatially sampled points to perform 2D Fourier transforms [8–11]. This is only possible with scanning laser Doppler vibrometers or air-coupled ultrasound technique for a sufficient wavenumber resolution. This procedure cannot be realised with reasonable effort using discrete sensors and is therefore limited in it's applicability.

In this study, a new framework for extracting GUW mode components from temporally sampled data is presented. It assumes a known dispersion relation, is based on only single sensor signals and uses frequency response functions (FRF) to describe the wave propagation in structures. To achieve this, sweep excitation is used for energy efficient determination of the structure's FRF between the actuation and sensing position. A transformation into the time domain results in impulse response functions (IRF) that are used to extract the respective mode components by a dispersion based extension of the frequency-domain intrinsic component decomposition (FICD) [12] and the iterative frequency-domain envelope-tracking filter (IFETF) [13].

FREQUENCY RESPONSE FUNCTIONS FOR GUW PROPAGATION

Assuming broadband GUW excitation $f(t)$ at the actuator position and linear wave propagation, the response $u(t)$ at a given sensor position can be derived by convolving the excitation signal with the structure's IRF $h(t)$. The Fourier transform converts the signals to the frequency domain and transforms the IRF into the FRF $H(\omega)$:

$$u(t) = h(t) * f(t) \qquad \text{with} \qquad h(t) = \mathcal{F}^{-1}\{H(\omega)\} \tag{1}$$

$$U(\omega) = H(\omega) \cdot F(\omega) \qquad \text{with} \qquad H(\omega) = \mathcal{F}\{h(t)\} \tag{2}$$

In this work, only the fundamental S_0 and A_0 modes as well as no mode conversion

are considered. Thus, the wave propagation can be split into mode selective parts:

$$u(t) = u_{S_0}(t) + u_{A_0}(t) \quad = (h_{S_0}(t) + h_{A_0}(t)) * f(t) \tag{3}$$

$$U(\omega) = U_{S_0}(\omega) + U_{A_0}(\omega) = (H_{S_0}(\omega) + H_{A_0}(\omega)) \cdot F(\omega). \tag{4}$$

The aim of this work is to extract the mode selective IRFs and FRFs, respectively. This enables the calculation of the structure's virtual mode-selective response to any given excitation signal within the investigated frequency range.

FRAMEWORK FOR EXTRACTING MODE-SELECTIVE FRFS FROM TEMPORALLY SAMPLED, BROADBAND AND MULTIMODAL GUW DATA

Figure 1 depicts the framework for extracting mode-selective FRFs from temporally sampled, broadband and multimodal GUW data that is designed within this work. This framework takes two inputs: the dispersion relation data that is assumed to be known for the inspected structure and the FRF between the actuation and respective sensing position. For increased energy efficiency, the FRF is measured using sweep excitation and subsequently transformed into the IRF which is then truncated for reducing computational costs while keeping all structural information. Additionally, the IRF is used for mode extraction as the included components are significantly more exposed compared to the FRF, cf. Figure 2.

Dispersion Based Frequency-Domain Intrinsic Component Decomposition

In this framework, the group delays (GD) and generalised dispersive components (GDC), cf. [13], of every mode component are extracted with the IFETF algorithm [13]. This algorithm needs frequency-domain dispersive signals and initial GD estimates. To obtain the GD estimates, this work extends the FICD algorithm [12] by an optimization procedure that is based on the structure's dispersive relations.

The FICD algorithm is based on polynomial kernel functions to determine nonlinear GDs, but is not capable of extracting every type of ridge courses. Therefore it is extended by the new mode-selective dispersion based ridge extraction (MDBRE) method resulting in the dispersion based frequency-domain intrinsic component decomposition algorithm (DBFICD).

The main idea of the MDBRE method is to estimate the distance travelled $\tilde{x}_m$ by a wave component m within the structure. Knowing the dispersion relation, the structure's broadband response after any given distance can be calculated. If the estimated response to an ideal impulse fits to a component in the IRF, it is extracted and assigned to the respective corresponding mode.

The GD $\tilde{\boldsymbol{\tau}}_m(f)$ for a given distance can be calculated by

$$\tilde{\boldsymbol{\tau}}_{m,S_0/A_0}(f) = \tilde{x}_m / \boldsymbol{c}_{g,S_0/A_0}(f) \tag{5}$$

with known group velocity $\boldsymbol{c}_{g,S_0/A_0}(f)$ for both fundamental modes, respectively.

The cost function used within this framework to estimate $\tilde{x}_m$ aims at maximising the amplitude of the ridge in the time-frequency representation as well as an adapted

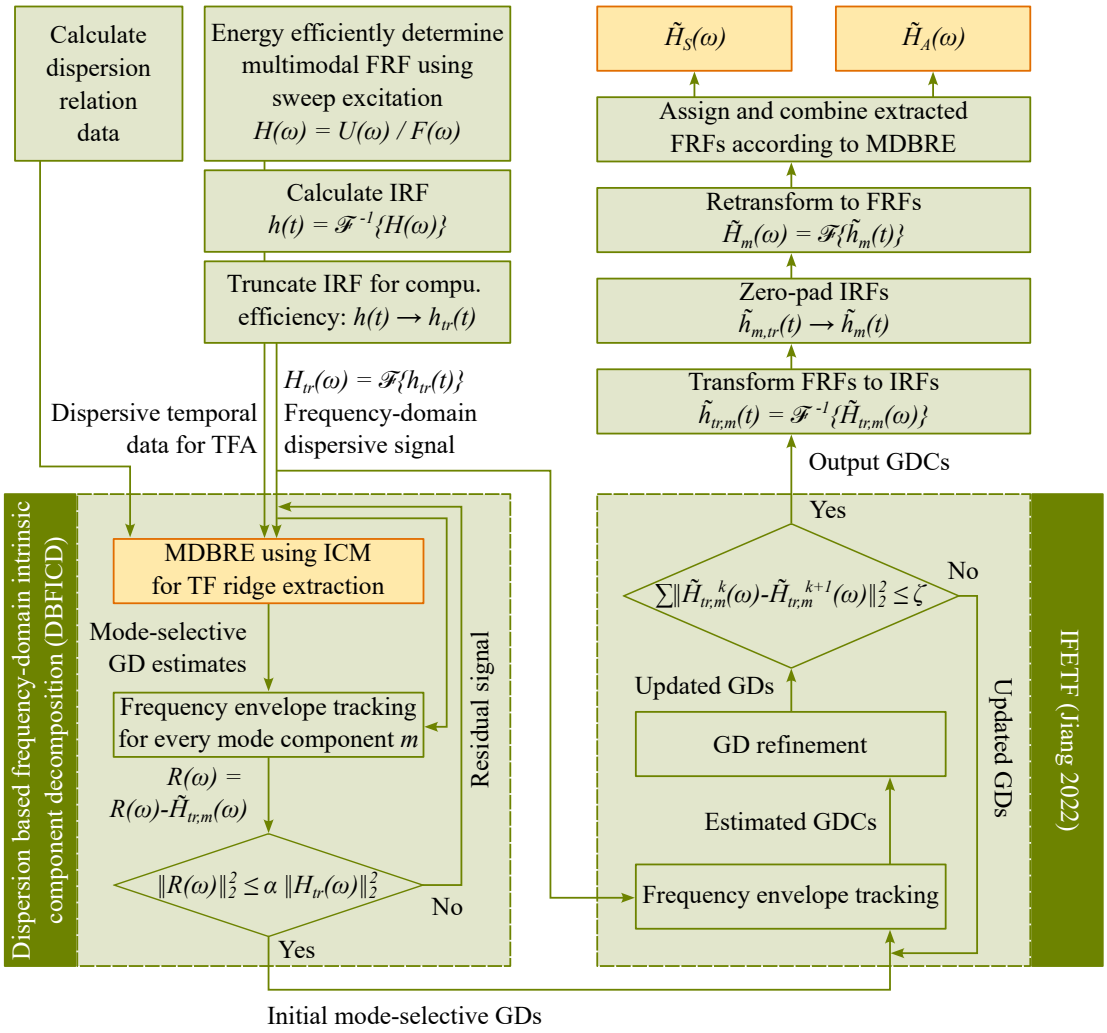

MDBRE: mode-selective dispersion based ridge extraction, TFA: time-frequency analysis,
ICM: impulse concentration measurement, GD: group delay, GDC: generalized dispersive component

Figure 1. Framework for mode-selective FRF decomposition based on DBFICD (an extension of the FICD algorithm [12]) and IFETF [13]. Figure adapted from [13].

version of the impulse concentration measurement (ICM) [12] that can be referred to as a criterion for the fit between the estimated and the actual ridge course. The cost function is defined as follows:

$$\tilde{x}_m = \underset{x_m}{\operatorname{argmax}} \left[\sum_f |\underline{\boldsymbol{V}}(\tilde{\boldsymbol{\tau}}_m(x_m, f), f)|^2 + \lambda \cdot max\left(|\mathcal{F}^{-1}\{\underline{\boldsymbol{H}}_{dem}(f, \tilde{\boldsymbol{\tau}}_m(x_m, f))\}|^p \right) \right]. \tag{6}$$

$\underline{\boldsymbol{V}}$ is the time-frequency representation of the signal obtained by the time-frequency analysis method of short-time Fourier transform (STFT) and λ is a penalty parameter to weight the importance of ridge amplitude and the second summand, the adpated version of the ICM. Here, $\mathcal{F}^{-1}$ denotes the inverse Fourier transform, $\underline{\boldsymbol{H}}_{dem}$ is the demodulated frequency-domain signal and p is a penalty parameter balancing the function values of the ICM.

The demodulation procedure removes the expected dispersion of the estimated mode from the signal based on the respective estimated GD $\tilde{\boldsymbol{\tau}}_m$:

$$\underline{\boldsymbol{H}}_{dem}(f, \tilde{\boldsymbol{\tau}}_m(f)) = \underline{\boldsymbol{H}}(f) \cdot e^{-\mathrm{j}\tilde{\boldsymbol{\varphi}}_m(f)} \tag{7}$$

with the phase $\tilde{\boldsymbol{\varphi}}_m(f)$ being related to the GD via

$$\tilde{\boldsymbol{\varphi}}_m(f) = -2\pi \int \tilde{\boldsymbol{\tau}}_m(f)\, df. \tag{8}$$

If the estimated GD coincides with the actual GD of a component, the dispersion is completely removed and the demodulation of the signal results in an impulse-like time-domain signal for the respective mode component. The higher the value of this temporal signal, the more accurate the GD estimate, cf. ICM [12].

To solve the optimisation problem, the global optimisation algorithm of dual annealing is used. In every component estimation iteration, Equation 6 is optimised for both modes using Equation 5 and the GD estimation for the mode with higher function value of the cost function is selected.

Similar to [12], a frequency envelope tracking for the corresponding mode component is performed to extract the respective GDC and extract it from the residual signal. Every iteration extracts a new GD estimation with corresponding GDC until the energy content of the residual signal falls below a defined threshold and the estimated GDs are transferred to the IFETF algorithm [13] to perform a GD refinement and extract the updated GDCs.

Final Extraction of Mode-Selective FRFs

After extracting the truncated versions of the FRFs, multiple Fourier transforms and zero-padding restore the initial frequency resolution, cf. Figure 1. The resulting FRFs are combined according to the mode assignment determined by the MDBRE method during the DBFICD algorithm. This results in two separate FRFs for the S_0 and A_0 mode, respectively, which enables a mode-selective evaluation of broadband, multimodal GUW data for SHM applications and damage detection.

NUMERICAL RESULTS

To validate the methods applicability, GUW propagation in a $3\,\mathrm{mm}$ aluminium plate (material: AW-6060) is generically modelled. Figure 2a shows the STFT of the structural response to a sweep excitation with linearly increasing frequency up to $1\,\mathrm{MHz}$. The respective wave components are simulated to travel for $1\,\mathrm{m}$, $2\,\mathrm{m}$ and $3\,\mathrm{m}$. Due to the long excitation duration, the ridges are very close to another which demonstrates, why a mode extraction from an FRF is difficult. Figure 2b however presents the STFT of the resulting and truncated IRF after performing an inverse Fourier transform of the FRF. It is evident that the duration with the same structural information is significantly shorter and the ridges are significantly better exposed for extraction while containing sufficient energy.

After performing the presented method illustrated in Figure 1, two mode-selective IRFs and thus FRFs are extracted from the modelled structural response to the sweep

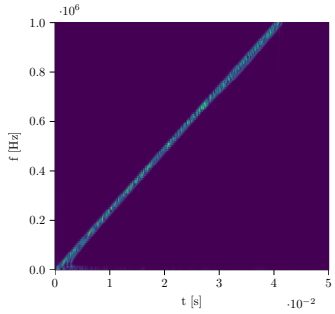

(a) STFT of num. sweep signal recorded at sensor and used for structural identification ($x = 1\,\mathrm{m}$, $2\,\mathrm{m}$ and $3\,\mathrm{m}$). Elongated signal with closely located, hard to be distinguished ridges.

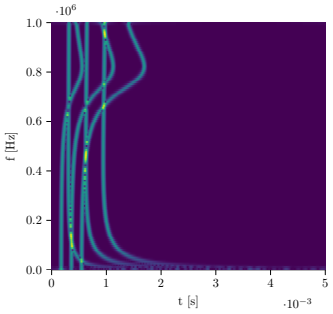

(b) STFT of num. resulting IRF ($x = 1\,\mathrm{m}$, $2\,\mathrm{m}$ and $3\,\mathrm{m}$). Truncated signal section with same information content as sweep and significantly better exposed ridges.

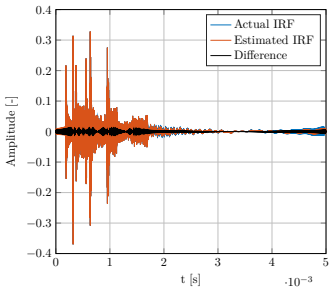

(c) Comparison between num. IRF and combination of extracted A_0 and S_0 IRF components. High quality reproduction of the initial IRF.

Figure 2. Numerically evaluated signals to visualise need for IRFs and quality assessment of IRF extraction method using DBFICD, MDBRE and IFETF, cf. Figure 1.

excitation. Figure 2c depicts a zoom into the comparison between actual IRF and the combined extracted IRFs. It is evident that the structural behaviour can successfully be reproduced with the presented framework.

In a next step, the applicability to real-world experimental data will be validated.

EXPERIMENTAL VALIDATION

The experimental validation aims to exemplary show the general applicability of the presented method to real data. Figure 3a shows the experimental setup used within this work. A $3\,\mathrm{mm}$ thick aluminium plate (material: AW-6060) is equipped with a two-sided actuator setup for mode-selective excitation. $0.7\,\mathrm{m}$ from the excitation position, the structural response is measured using a laser Doppler vibrometer. In the first run, only the top actuator is used to excite the structure with a sweep signal with linearly increasing frequency from $50\,\mathrm{kHz}$ to $350\,\mathrm{kHz}$ to determine the structure's multimodal FRF and IRF in the given frequency range. In the second run, the two actuators are excited asymmetrically with a 5 cycle Hanning-windowed burst with a centre frequency of $200\,\mathrm{kHz}$ for a physical mode-selective excitation of the A_0 mode. The aim is to extract the IRF corresponding to the A_0 mode from the multimodal signal from the first run and compare the virtually calculated to the physical mode-selective response.

Due to limitations in programmatic efficiency and computational resources, the distances travelled are estimated by graphical evaluation in this case, which is currently under improvement. Performing the FRF extraction with the framework presented within this work results in an IRF and consequently an FRF per S_0 and A_0 mode.

Figure 3b visualises the structural response to the physical mode-selective asymmetric excitation and the virtually calculated response $u_{virt,A_0}(t)$ to the same excitation signal. Here, $u_{virt,A_0}(t) = \mathcal{F}^{-1}\{U_{virt,A_0}(\omega)\}$ with $U_{virt,A_0}(\omega) = H_{extracted,A_0}(\omega) \cdot F(\omega)$. The plot shows a reasonable agreement between the actual and virtual response with

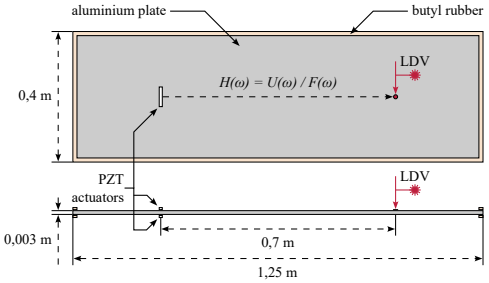

(a) Experimental setup for multimodal and mode-selective excitation and contact-free sensing of GUW using laser Doppler vibrometer (LDV).

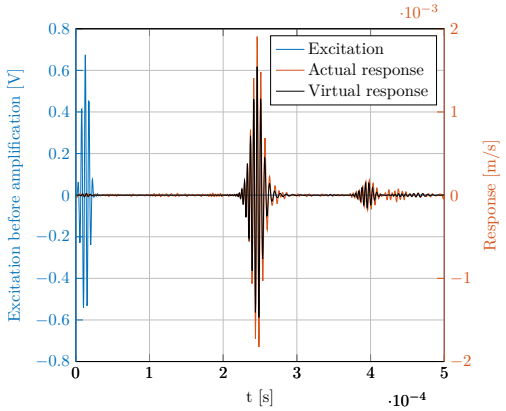

(b) Comparison of physical structural response to mode-selective, asymmetric excitation with 200 kHz Hanning-windowed burst signal and virtual response calculated with extracted A_0 FRF via $U_{virt,A_0}(\omega) = H_{extracted,A_0}(\omega) \cdot F(\omega)$.

Figure 3. Experimental investigation to validate the method's applicability.

only minor deviations. An improvement of the approximation is expected with increased programmatic efficiency and further optimisation of the parameters used within the DB-FICD and IFETF algorithm.

As has been shown, the presented method enables mode-selective extraction of mode components from a broadband multimodal GUW signal for both fundamental modes and in a wide frequency range depending only on the realisable excitation signal.

CONCLUSION

The presented concept for generating mode-selective FRFs from temporally sampled, single sensor, broadband and multimodal guided ultrasonic wave signals is validated numerically and experimentally. It enables SHM systems to work with multimodal excitation, which reduces the setup complexity and increases the application range by providing information for both fundamental modes over a wide frequency range.

Future work will assess the robustness of the method to noise, closely spaced ridges, etc. Additionally, mode conversion and anisotropic media will be addressed. Afterwards, the applicability of this method for damage detection with phased array systems based on FRFs [4, 6] will be investigated, where multimodal signals significantly reduce the algorithm's performance.

ACKNOWLEDGMENT

The authors expressly acknowledge the financial support for the research work on this article within the Research Unit 3022 "Ultrasonic Monitoring of Fibre Metal Laminates Using Integrated Sensors" (Project number: 418311604) by the German Research Foundation (Deutsche Forschungsgemeinschaft (DFG)).

REFERENCES

1. Lammering, R., U. Gabbert, M. Sinapius, T. Schuster, and P. Wierach, eds. 2018. *Lamb-Wave Based Structural Health Monitoring in Polymer Composites*, Springer eBook Collection, Springer, Cham, doi:10.1007/978-3-319-49715-0.
2. Giurgiutiu, V. 2008. *Structural health monitoring with piezoelectric wafer active sensors*, Academic Press/Elsevier, Amsterdam, ISBN 9786611099992.
3. Rose, J. L. 2014. *Ultrasonic guided waves in solid media*, Cambridge University Press, Cambridge, doi:10.1017/CBO9781107273610.
4. Lang, Y.-F., S.-H. Tian, Z.-B. Yang, W. Zhang, D.-T. Kong, K.-L. Xu, and X.-F. Chen. 2022. "Focusing phase imaging for Lamb wave phased array," *Smart Materials and Structures*, 31(2), doi:10.1088/1361-665X/ac40e0.
5. Yu, L. and V. Giurgiutiu. 2007. "In-situ optimized PWAS phased arrays for Lamb wave structural health monitoring," *Journal of Mechanics of Materials and Structures*, 2(3):459–487, ISSN 1559-3959, doi:10.2140/jomms.2007.2.459.
6. Yang, Z.-B., M.-F. Zhu, Y.-F. Lang, and X.-F. Chen. 2022. "FRF-based lamb wave phased array," *Mechanical Systems and Signal Processing*, 166, doi:10.1016/j.ymssp.2021.108462.
7. Xu, C., H. Zuo, and M. Deng. 2022. "Dispersive MUSIC algorithm for Lamb wave phased array," *Smart Materials and Structures*, 31(2), doi:10.1088/1361-665X/ac4874.
8. Gao, F., L. Zeng, J. Lin, and Z. Luo. 2017. "Mode separation in frequency–wavenumber domain through compressed sensing of far-field Lamb waves," *Measurement Science and Technology*, 28(7):075004, doi:10.1088/1361-6501/aa6c54.
9. Michaels, T. E., J. E. Michaels, and M. Ruzzene. 2011. "Frequency-wavenumber domain analysis of guided wavefields," *Ultrasonics*, 51(4):452–466, doi:10.1016/j.ultras.2010.11.011.
10. Roloff, T., R. Mitkus, J. N. Lion, and M. Sinapius. 2022. "3D-Printable Piezoelectric Composite Sensors for Acoustically Adapted Guided Ultrasonic Wave Detection," *Sensors*, 22(18):6964, doi:10.3390/s22186964.
11. Tian, Z. and L. Yu. 2014. "Lamb wave frequency–wavenumber analysis and decomposition," *Journal of Intelligent Material Systems and Structures*, 25(9):1107–1123, doi:10.1177/1045389X14521875.
12. Liu, Z., Q. He, S. Chen, X. Dong, Z. Peng, and W. Zhang. 2019. "Frequency-domain intrinsic component decomposition for multimodal signals with nonlinear group delays," *Signal Processing*, 154:57–63, doi:10.1016/j.sigpro.2018.07.026.
13. Jiang, Y. and G. Niu. 2022. "An iterative frequency-domain envelope-tracking filter for dispersive signal decomposition in structural health monitoring," *Mechanical Systems and Signal Processing*, 179:1–26, doi:10.1016/j.ymssp.2022.109329.